Spherical signal processing for cosmology

Jason McEwen
http://www.jasonmcewen.org/

Department of Physics and Astronomy,
University College London (UCL)

Signal Processing for the Physical Sciences
The Kavli Royal Society International Centre
March 2012

Outline

1. Cosmology
   - Big Bang
   - Cosmic microwave background
2. Harmonic analysis on the sphere
   - Spherical harmonic transform
   - Sampling theorems
3. Compressive sensing on the sphere
   - Compressive sensing
   - TV inpainting
   - Simulations
4. Wavelets on the sphere
   - Recap Euclidean wavelets
   - Continuous wavelets
   - Scale-discretised wavelets
5. Wavelets on the ball
   - Scale-discretised wavelets

Outline

1. Cosmology
   - Big Bang
   - Cosmic microwave background
2. Harmonic analysis on the sphere
   - Spherical harmonic transform
   - Sampling theorems
3. Compressive sensing on the sphere
   - Compressive sensing
   - TV inpainting
   - Simulations
4. Wavelets on the sphere
   - Recap Euclidean wavelets
   - Continuous wavelets
   - Scale-discretised wavelets
5. Wavelets on the ball
   - Scale-discretised wavelets

Cosmological concordance model

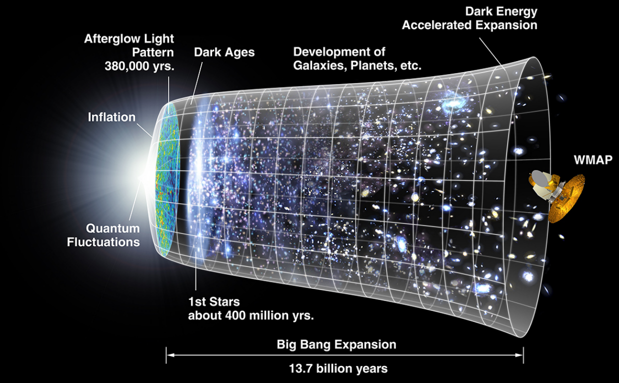

Credit: WMAP Science Team

Observations of the cosmic microwave background (CMB)

- Full-sky observations of the CMB ongoing.

(a) COBE (launched 1989)

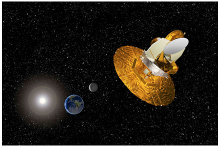

(b) WMAP (launched 2001)

(c) Planck (launched 2009)

- Each new experiment provides dramatic improvement in precision and resolution of observations.

(cobe 2 wmap movie)

(planck movie)

(d) COBE to WMAP [Credit: WMAP Science Team]

(e) Planck observing strategy [Credit: Planck Collaboration]

Cosmic microwave background (CMB)

- Temperature of early Universe sufficiently hot that photons had enough energy to ionise hydrogen.
- Compton scattering happened frequently $\Rightarrow$ mean free path of photons extremely small.
- Universe consisted of an opaque photon-baryon fluid.
- As Universe expanded it cooled, until majority of photons no longer had sufficient energy to ionise hydrogen.
- Photons decoupled from baryons and the Universe became essentially transparent to radiation.
- *Recombination* occurred when temperature of Universe dropped to 3000K ($\sim$400,000 years after the Big Bang).
- Photons then free to propagate largely unhindered and observed today on celestial sphere as CMB radiation.
- CMB is highly uniform over the celestial sphere, however it contains small fluctuations at a relative level of 10^{-5} due to acoustic oscillations in the early Universe.
- CMB observed on spherical manifold, hence the geometry of the sphere must be taken into account in any analysis.

Cosmic microwave background (CMB)

- Temperature of early Universe sufficiently hot that photons had enough energy to ionise hydrogen.
- Compton scattering happened frequently $\Rightarrow$ mean free path of photons extremely small.
- Universe consisted of an opaque photon-baryon fluid.
- As Universe expanded it cooled, until majority of photons no longer had sufficient energy to ionise hydrogen.
- Photons decoupled from baryons and the Universe became essentially transparent to radiation.
- *Recombination* occurred when temperature of Universe dropped to 3000K ($\sim$400,000 years after the Big Bang).
- Photons then free to propagate largely unhindered and observed today on celestial sphere as CMB radiation.
- CMB is highly uniform over the celestial sphere, however it contains small fluctuations at a relative level of 10^{-5} due to acoustic oscillations in the early Universe.
- CMB observed on spherical manifold, hence the geometry of the sphere must be taken into account in any analysis.

Cosmic microwave background (CMB)

- Temperature of early Universe sufficiently hot that photons had enough energy to ionise hydrogen.
- Compton scattering happened frequently $\Rightarrow$ mean free path of photons extremely small.
- Universe consisted of an opaque photon-baryon fluid.
- As Universe expanded it cooled, until majority of photons no longer had sufficient energy to ionise hydrogen.
- Photons decoupled from baryons and the Universe became essentially transparent to radiation.
- *Recombination* occurred when temperature of Universe dropped to 3000K ($\sim$400,000 years after the Big Bang).

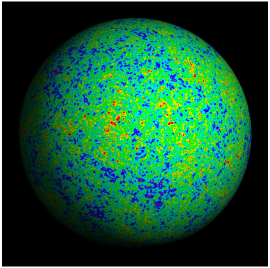

Credit: Max Tegmark

- Photons then free to propagate largely unhindered and observed today on celestial sphere as CMB radiation.
- CMB is highly uniform over the celestial sphere, however it contains small fluctuations at a relative level of 10^{-5} due to acoustic oscillations in the early Universe.
- CMB observed on spherical manifold, hence the geometry of the sphere must be taken into account in any analysis.

Cosmic microwave background (CMB)

- Quantum fluctuations in the early Universe blown to macroscopic scales by inflation, establishing acoustic oscillations in primordial plasma of the very early Universe.
- Provide the seeds of structure formation in our Universe.
- Cosmological concordance model explains the power spectrum of these oscillations to very high precision.

- Although a general cosmological concordance model is now established, many details remain unclear. Study of more exotic cosmological models now important.

Cosmic microwave background (CMB)

- Quantum fluctuations in the early Universe blown to macroscopic scales by inflation, establishing acoustic oscillations in primordial plasma of the very early Universe.
- Provide the seeds of structure formation in our Universe.
- Cosmological concordance model explains the power spectrum of these oscillations to very high precision.

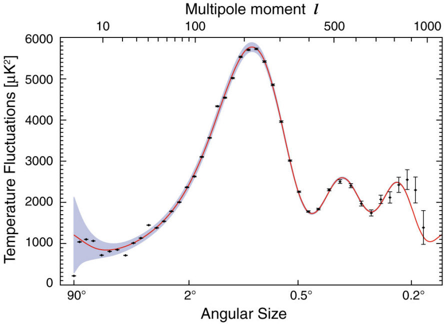

Credit: WMAP Science Team

- Although a general cosmological concordance model is now established, many details remain unclear. Study of more exotic cosmological models now important.

Cosmic microwave background (CMB)

- Quantum fluctuations in the early Universe blown to macroscopic scales by inflation, establishing acoustic oscillations in primordial plasma of the very early Universe.
- Provide the seeds of structure formation in our Universe.
- Cosmological concordance model explains the power spectrum of these oscillations to very high precision.

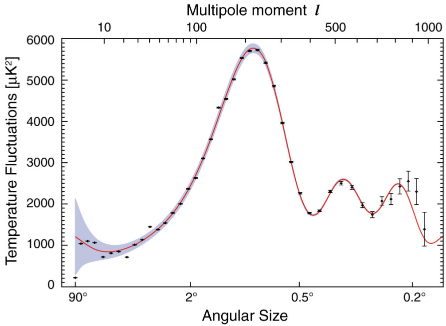

Credit: WMAP Science Team

- Although a general cosmological concordance model is now established, many details remain unclear. Study of more exotic cosmological models now important.

Observations on the sphere

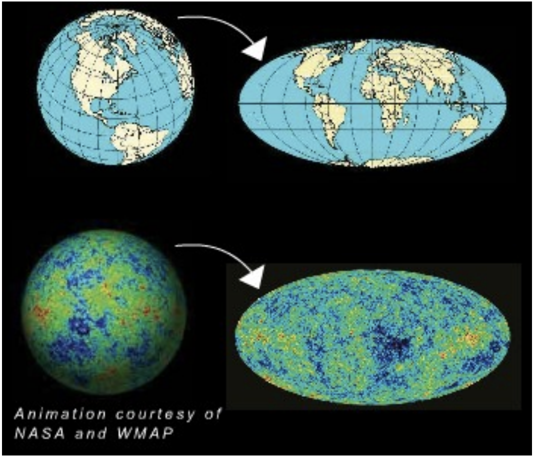

Credit: Alec MacAndrew

Outline

Spherical harmonic transform

- The spherical harmonics are the eigenfunctions of the Laplacian on the sphere: $\Delta_{S^2} Y_{\ell m} = -\ell(\ell+1) Y_{\ell m}$.

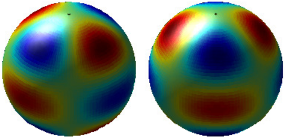

(f) $\ell = 4, m = 2$

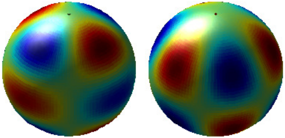

(g) $\ell = 4, m = 3$

Figure: Spherical harmonic functions (real and imaginary parts).

- Any square integrable scalar function on the sphere $f \in L^2(S^2)$ may be represented by its spherical harmonic expansion:

$$f(\theta, \varphi) = \sum_{\ell=0}^{\infty} \sum_{m=-\ell}^{\ell} f_{\ell m} \, Y_{\ell m}(\theta, \varphi) .$$

- The spherical harmonic coefficients are given by the usual projection onto each basis function:

$$f_{\ell m} = \langle f, \, Y_{\ell m} \rangle = \int_{S^2} d\Omega(\theta, \varphi) \, f(\theta, \varphi) \, Y_{\ell m}^*(\theta, \varphi) .$$

Spherical harmonic transform

- The spherical harmonics are the eigenfunctions of the Laplacian on the sphere: $\Delta_{\mathrm{S}^2} Y_{\ell m} = -\ell(\ell+1) Y_{\ell m}$.

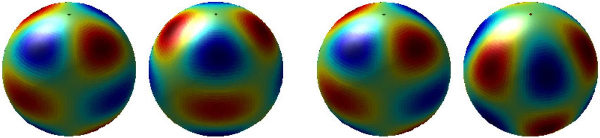

(a) $\ell = 4, m = 2$ (b) $\ell = 4, m = 3$

Figure: Spherical harmonic functions (real and imaginary parts).

- Any square integrable scalar function on the sphere $f \in \mathrm{L}^2(\mathrm{S}^2)$ may be represented by its spherical harmonic expansion:

$$f(\theta, \varphi) = \sum_{\ell=0}^{\infty} \sum_{m=-\ell}^{\ell} f_{\ell m} \, Y_{\ell m}(\theta, \varphi) \, .$$

- The spherical harmonic coefficients are given by the usual projection onto each basis function:

$$f_{\ell m} = \langle f, \, Y_{\ell m} \rangle = \int_{\mathrm{S}^2} \mathrm{d}\Omega(\theta, \varphi) \, f(\theta, \varphi) \, Y_{\ell m}^*(\theta, \varphi) \, .$$

Spherical harmonic transform

- We consider signals on the sphere band-limited at L, that is signals such that $f_{\ell m} = 0, \forall \ell \geq L$
  $\Rightarrow$ summations may be truncated at $L-1$:

$$f(\theta, \varphi) = \sum_{\ell=0}^{L-1} \sum_{m=-\ell}^{\ell} f_{\ell m} \, Y_{\ell m}(\theta, \varphi) \, .$$

- For a band-limited signal, can we compute $f_{\ell m}$ exactly?
  $\rightarrow$ Sampling theorems on the sphere.

- Aside: Generalise to spin functions on the sphere.

  Square integrable spin functions on the sphere ${}_s f \in \mathrm{L}^2(\mathbb{S}^2)$, with integer spin $s \in \mathbb{Z}$, are defined by their behaviour under local rotations. By definition, a spin function transforms as

$${}_s f'(\theta, \varphi) = \mathrm{e}^{-\mathrm{i} s \chi} \, {}_s f(\theta, \varphi)$$

  under a local rotation by χ, where the prime denotes the rotated function.

Spherical harmonic transform

- We consider signals on the sphere band-limited at L, that is signals such that $f_{\ell m} = 0, \forall \ell \geq L$
$\Rightarrow$ summations may be truncated at $L-1$:

$$f(\theta, \varphi) = \sum_{\ell=0}^{L-1} \sum_{m=-\ell}^{\ell} f_{\ell m}\, Y_{\ell m}(\theta, \varphi)\ .$$

- For a band-limited signal, can we compute $f_{\ell m}$ exactly?
$\rightarrow$ Sampling theorems on the sphere.

- Aside: Generalise to spin functions on the sphere.

Square integrable spin functions on the sphere ${}_s f \in \mathrm{L}^2(\mathrm{S}^2)$, with integer spin $s \in \mathbb{Z}$, are defined by their behaviour under local rotations. By definition, a spin function transforms as

$${}_s f'(\theta, \varphi) = \mathrm{e}^{-\mathrm{i} s \chi}\ {}_s f(\theta, \varphi)$$

under a local rotation by χ, where the prime denotes the rotated function.

Spherical harmonic transform

- We consider signals on the sphere band-limited at L, that is signals such that $f_{\ell m} = 0, \forall \ell \geq L$
  $\Rightarrow$ summations may be truncated at $L-1$:

$$f(\theta, \varphi) = \sum_{\ell=0}^{L-1} \sum_{m=-\ell}^{\ell} f_{\ell m} \, Y_{\ell m}(\theta, \varphi) \, .$$

- For a band-limited signal, can we compute $f_{\ell m}$ exactly?
  $\rightarrow$ Sampling theorems on the sphere.

- Aside: Generalise to spin functions on the sphere.

  Square integrable spin functions on the sphere ${}_sf \in \mathrm{L}^2(\mathrm{S}^2)$, with integer spin $s \in \mathbb{Z}$, are defined by their behaviour under local rotations. By definition, a spin function transforms as

$$ {}_sf'(\theta, \varphi) = \mathrm{e}^{-\mathrm{i}s\chi} \, {}_sf(\theta, \varphi)$$

  under a local rotation by χ, where the prime denotes the rotated function.

Driscoll & Healy sampling theorem (DH)

- Canonical sampling theorem on the sphere dervied by Driscoll & Healy (1994) for equiangular grids.
- Gives an explicit quadrature rule for the spherical harmonic transform:

$$f_{\ell m} = \sum_{t=0}^{2L-1} \sum_{p=0}^{2L-1} q_{\text{DH}}(\theta_t)\, f(\theta_t, \varphi_p)\, Y_{\ell m}^*(\theta_t, \varphi_p) ,$$

where the sample positions are defined by $\theta_t = \pi t / 2L$, for $t = 0, \ldots, 2L-1$, and $\varphi_p = \pi p / L$, for $p = 0, \ldots, 2L-1$

$\Rightarrow$ $N_{\text{DH}} = (2L-1)2L + 1 \sim 4L^2$ samples on the sphere.

- The quadrature weights are defined implicitly by the solution to

$$\sum_{t=0}^{2L-1} q_{\text{DH}}(\theta_t)\, P_\ell(\cos\theta_t) = \frac{2\pi}{L}\,\delta_{\ell 0} , \quad \forall \ell < 2L ,$$

and are given explicitly by

$$q_{\text{DH}}(\theta_t) = \frac{2\pi}{L^2}\, \sin\theta_t \sum_{k=0}^{L-1} \frac{\sin((2k+1)\theta_t)}{2k+1} .$$

Driscoll & Healy sampling theorem (DH)

- Canonical sampling theorem on the sphere dervied by Driscoll & Healy (1994) for equiangular grids.
- Gives an explicit quadrature rule for the spherical harmonic transform:

$$f_{\ell m} = \sum_{t=0}^{2L-1} \sum_{p=0}^{2L-1} q_{\text{DH}}(\theta_t) \, f(\theta_t, \varphi_p) \, Y_{\ell m}^*(\theta_t, \varphi_p) \ ,$$

where the sample positions are defined by $\theta_t = \pi t / 2L$, for $t = 0, \ldots, 2L-1$, and $\varphi_p = \pi p / L$, for $p = 0, \ldots, 2L-1$

$\Rightarrow$ $N_{\text{DH}} = (2L-1)2L + 1 \sim 4L^2$ samples on the sphere.

- The quadrature weights are defined implicitly by the solution to

$$\sum_{t=0}^{2L-1} q_{\text{DH}}(\theta_t) \, P_\ell(\cos\theta_t) = \frac{2\pi}{L} \, \delta_{\ell 0} \ , \quad \forall \ell < 2L \ ,$$

and are given explicitly by

$$q_{\text{DH}}(\theta_t) = \frac{2\pi}{L^2} \, \sin\theta_t \sum_{k=0}^{L-1} \frac{\sin((2k+1)\theta_t)}{2k+1} \ .$$

A new sampling theorem

- A new sampling theorem (with fast algorithms) has emerged very recently by performing a factoring of rotations and then by associating the sphere with the torus through a periodic extension.
- Similar to making a periodic extension in θ of a function f on the sphere.
- First suggested by Risbo (1996) and Wandelt & Gorski (2001) for the inverse spherical harmonic transform.

A new sampling theorem

- A new sampling theorem (with fast algorithms) has emerged very recently by performing a factoring of rotations and then by associating the sphere with the torus through a periodic extension.
- Similar to making a periodic extension in θ of a function f on the sphere.

(a) Function on sphere (b) Even function on torus (c) Odd function on torus

Figure: Associating functions on the sphere and torus

- First suggested by Risbo (1996) and Wandelt & Gorski (2001) for the inverse spherical harmonic transform.

A new sampling theorem

- A new sampling theorem (with fast algorithms) has emerged very recently by performing a factoring of rotations and then by associating the sphere with the torus through a periodic extension.
- Similar to making a periodic extension in θ of a function f on the sphere.

(a) Function on sphere (b) Even function on torus (c) Odd function on torus

Figure: Associating functions on the sphere and torus

- First suggested by Risbo (1996) and Wandelt & Gorski (2001) for the inverse spherical harmonic transform.

A new sampling theorem

Inverse spherical harmonic transform

$$ {}_sf(\theta, \varphi) = \sum_{m=-(L-1)}^{L-1} {}_sF_m(\theta)\, e^{im\varphi} $$

$$ {}_sF_m(\theta) = \sum_{m'=-(L-1)}^{L-1} {}_sF_{mm'}\, e^{im'\theta} $$

$$ {}_sF_{mm'} = (-1)^s\, i^{-(m+s)} \sum_{\ell=0}^{L-1} \sqrt{\frac{2\ell+1}{4\pi}}\, \Delta^{\ell}_{m'm}\, \Delta^{\ell}_{m',-s}\, {}_sf_{\ell m} $$

- JDM (2011a), *Fast, exact (but unstable) spin spherical harmonic transforms*
  - Even and odd periodic extensions.
  - Numerically *unstable* forward transform at modest band-limits ($L \sim 32$)!
- Huffenberger & Wandelt (2010), *Fast and exact spin-s spherical harmonic transforms*
  - Merged even and odd periodic extensions by applying a shift by π in φ.
  - Numerically *stable* by substituting the Fourier series expression for ${}_sf$ in the forward transform to develop a quadrature!
- JDM & Wiaux (2011b), *A novel sampling theorem on the sphere*
  - Performed the periodic extension in the Fourier transform of ${}_sf$ in φ.
  - Reduced the number of samples by a factor of two!

A new sampling theorem

Inverse spherical harmonic transform

$$ {}_sf(\theta, \varphi) = \sum_{m=-(L-1)}^{L-1} {}_sF_m(\theta)\, e^{im\varphi} $$

$$ {}_sF_m(\theta) = \sum_{m'=-(L-1)}^{L-1} {}_sF_{mm'}\, e^{im'\theta} $$

$$ {}_sF_{mm'} = (-1)^s\, i^{-(m+s)} \sum_{\ell=0}^{L-1} \sqrt{\frac{2\ell+1}{4\pi}}\, \Delta^{\ell}_{m'm}\, \Delta^{\ell}_{m',-s}\, {}_sf_{\ell m} $$

- JDM (2011a), *Fast, exact (but unstable) spin spherical harmonic transforms*
  - Even and odd periodic extensions.
  - Numerically *unstable* forward transform at modest band-limits ($L \sim 32$)!
- Huffenberger & Wandelt (2010), *Fast and exact spin-s spherical harmonic transforms*
  - Merged even and odd periodic extensions by applying a shift by π in φ.
  - Numerically *stable* by substituting the Fourier series expression for ${}_sf$ in the forward transform to develop a quadrature!

- JDM & Wiaux (2011b), *A novel sampling theorem on the sphere*
  - Performed the periodic extension in the Fourier transform of ${}_sf$ in φ.
  - Reduced the number of samples by a factor of two!

A new sampling theorem

- Properties:
  - Equiangular pixelisation of the sphere
  - Require $\sim 2L^2$ samples on the sphere
  - Exploit fast Fourier transforms to yield a fast algorithm with complexity $\mathcal{O}(L^3)$
  - No precomputation and very flexible regarding use of Wigner recursions
  - Extends to spin function on the sphere with no change in complexity or computation time

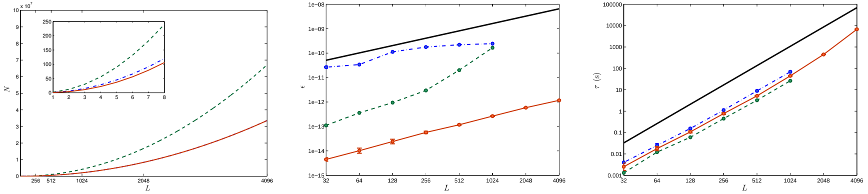

(a) Number of samples (b) Numerical accuracy (c) Computation time

Figure: Performance of various sampling theorems (DH sampling theorem; new sampling theorem)

Outline

Compressive sensing on the sphere

- A reduction in the number of samples required to represent a band-limited signal on the sphere has important implications for compressive sensing.
- Many natural signals are sparse in dictionaries with atoms position on each grid point through a convolution, for example in wavelets frames, or in other measures defined directly in the spatial domain, such as in the magnitude of their gradient.
- A more efficient sampling of a band-limited signal on the sphere improves both the dimensionality and sparsity of the signal in the spatial domain.
- For a given number of measurements, a more efficient sampling theorem improves the quality of compressive sampling reconstruction.
- Illustrate with a total variation (TV) inpainting problem on the sphere.

Compressive sensing on the sphere

- A reduction in the number of samples required to represent a band-limited signal on the sphere has important implications for compressive sensing.
- Many natural signals are sparse in dictionaries with atoms position on each grid point through a convolution, for example in wavelets frames, or in other measures defined directly in the spatial domain, such as in the magnitude of their gradient.
- A more efficient sampling of a band-limited signal on the sphere improves both the dimensionality and sparsity of the signal in the spatial domain.
- For a given number of measurements, a more efficient sampling theorem improves the quality of compressive sampling reconstruction.
- Illustrate with a total variation (TV) inpainting problem on the sphere.

Compressive sensing on the sphere

- A reduction in the number of samples required to represent a band-limited signal on the sphere has important implications for compressive sensing.
- Many natural signals are sparse in dictionaries with atoms position on each grid point through a convolution, for example in wavelets frames, or in other measures defined directly in the spatial domain, such as in the magnitude of their gradient.
- A more efficient sampling of a band-limited signal on the sphere improves both the dimensionality and sparsity of the signal in the spatial domain.
- For a given number of measurements, a more efficient sampling theorem improves the quality of compressive sampling reconstruction.
- Illustrate with a total variation (TV) inpainting problem on the sphere.

Compressive sensing on the sphere

- A reduction in the number of samples required to represent a band-limited signal on the sphere has important implications for compressive sensing.
- Many natural signals are sparse in dictionaries with atoms position on each grid point through a convolution, for example in wavelets frames, or in other measures defined directly in the spatial domain, such as in the magnitude of their gradient.
- A more efficient sampling of a band-limited signal on the sphere improves both the dimensionality and sparsity of the signal in the spatial domain.
- For a given number of measurements, a more efficient sampling theorem improves the quality of compressive sampling reconstruction.
- Illustrate with a total variation (TV) inpainting problem on the sphere.

TV inpainting

- Consider inpainting problem $\boldsymbol{y} = \Phi \boldsymbol{x} + \boldsymbol{n}$ in the context of different sampling theorems, where:
  - the samples of f are denoted by the concatenated vector $\boldsymbol{x} \in \mathbb{R}^N$;
  - N is the number of samples on the sphere of the chosen sampling theorem;
  - M noisy measurements $\boldsymbol{y} \in \mathbb{R}^M$ are acquired;
  - the measurement operator $\Phi \in \mathbb{R}^{M \times N}$ represents a random masking of the signal;
  - the noise $\boldsymbol{n} \in \mathbb{R}^M$ is assumed to be iid Gaussian with zero mean.
- Define TV norm on the sphere:

$$\int_{\mathbb{S}^2} \mathrm{d}\Omega \, |\nabla f| \simeq \sum_{t=0}^{N_\theta - 1} \sum_{p=0}^{N_\varphi - 1} |\nabla f| \, q(\theta_t) \simeq \sum_{t=0}^{N_\theta - 1} \sum_{p=0}^{N_\varphi - 1} \sqrt{q^2(\theta_t)(\delta_\theta \boldsymbol{x})^2 + \frac{q^2(\theta_t)}{\sin^2 \theta_t}(\delta_\varphi \boldsymbol{x})^2} \equiv \|\boldsymbol{x}\|_{\mathrm{TV}} .$$

- TV inpainting problem solved directly on the sphere:

$$\boldsymbol{x}^\star = \underset{\boldsymbol{x}}{\arg\min} \, \|\boldsymbol{x}\|_{\mathrm{TV}} \ \text{ such that } \ \|\boldsymbol{y} - \Phi \boldsymbol{x}\|_2 \leq \epsilon .$$

- TV inpainting problem solved in harmonic space:

$$\hat{\boldsymbol{x}}^\star = \underset{\hat{\boldsymbol{x}}}{\arg\min} \, \|\Psi \hat{\boldsymbol{x}}\|_{\mathrm{TV}} \ \text{ such that } \ \|\boldsymbol{y} - \Phi \Psi \hat{\boldsymbol{x}}\|_2 \leq \epsilon ,$$

where Ψ represents the inverse spherical harmonic transform and harmonic coefficients are represented by the concatenated vector $\hat{\boldsymbol{x}} \in \mathbb{C}^{L^2}$.

TV inpainting

- Consider inpainting problem $\boldsymbol{y} = \Phi \boldsymbol{x} + \boldsymbol{n}$ in the context of different sampling theorems, where:
  - the samples of f are denoted by the concatenated vector $\boldsymbol{x} \in \mathbb{R}^N$;
  - N is the number of samples on the sphere of the chosen sampling theorem;
  - M noisy measurements $\boldsymbol{y} \in \mathbb{R}^M$ are acquired;
  - the measurement operator $\Phi \in \mathbb{R}^{M \times N}$ represents a random masking of the signal;
  - the noise $\boldsymbol{n} \in \mathbb{R}^M$ is assumed to be iid Gaussian with zero mean.
- Define TV norm on the sphere:

$$\int_{\mathbb{S}^2} \mathrm{d}\Omega \, |\nabla f| \simeq \sum_{t=0}^{N_\theta - 1} \sum_{p=0}^{N_\varphi - 1} |\nabla f| \, q(\theta_t) \simeq \sum_{t=0}^{N_\theta - 1} \sum_{p=0}^{N_\varphi - 1} \sqrt{q^2(\theta_t)(\delta_\theta \boldsymbol{x})^2 + \frac{q^2(\theta_t)}{\sin^2 \theta_t}(\delta_\varphi \boldsymbol{x})^2} \equiv \|\boldsymbol{x}\|_{\mathrm{TV}} \, .$$

- TV inpainting problem solved directly on the sphere:

$$\boldsymbol{x}^\star = \underset{\boldsymbol{x}}{\arg\min} \, \|\boldsymbol{x}\|_{\mathrm{TV}} \;\; \text{such that} \;\; \|\boldsymbol{y} - \Phi \boldsymbol{x}\|_2 \leq \epsilon \, .$$

- TV inpainting problem solved in harmonic space:

$$\hat{\boldsymbol{x}}^\star = \underset{\hat{\boldsymbol{x}}}{\arg\min} \, \|\Psi \hat{\boldsymbol{x}}\|_{\mathrm{TV}} \;\; \text{such that} \;\; \|\boldsymbol{y} - \Phi \Psi \hat{\boldsymbol{x}}\|_2 \leq \epsilon \, ,$$

where Ψ represents the inverse spherical harmonic transform and harmonic coefficients are represented by the concatenated vector $\hat{\boldsymbol{x}} \in \mathbb{C}^{L^2}$.

TV inpainting

- Consider inpainting problem $\boldsymbol{y} = \Phi \boldsymbol{x} + \boldsymbol{n}$ in the context of different sampling theorems, where:
  - the samples of f are denoted by the concatenated vector $\boldsymbol{x} \in \mathbb{R}^N$;
  - N is the number of samples on the sphere of the chosen sampling theorem;
  - M noisy measurements $\boldsymbol{y} \in \mathbb{R}^M$ are acquired;
  - the measurement operator $\Phi \in \mathbb{R}^{M \times N}$ represents a random masking of the signal;
  - the noise $\boldsymbol{n} \in \mathbb{R}^M$ is assumed to be iid Gaussian with zero mean.
- Define TV norm on the sphere:

$$\int_{\mathbb{S}^2} \mathrm{d}\Omega \, |\nabla f| \simeq \sum_{t=0}^{N_\theta - 1} \sum_{p=0}^{N_\varphi - 1} |\nabla f| \, q(\theta_t) \simeq \sum_{t=0}^{N_\theta - 1} \sum_{p=0}^{N_\varphi - 1} \sqrt{q^2(\theta_t)(\delta_\theta \boldsymbol{x})^2 + \frac{q^2(\theta_t)}{\sin^2 \theta_t}(\delta_\varphi \boldsymbol{x})^2} \equiv \|\boldsymbol{x}\|_{\mathrm{TV}} \, .$$

- TV inpainting problem solved directly on the sphere:

$$\boldsymbol{x}^\star = \underset{\boldsymbol{x}}{\arg\min} \, \|\boldsymbol{x}\|_{\mathrm{TV}} \text{ such that } \|\boldsymbol{y} - \Phi \boldsymbol{x}\|_2 \leq \epsilon \, .$$

- TV inpainting problem solved in harmonic space:

$$\hat{\boldsymbol{x}}^\star = \underset{\hat{\boldsymbol{x}}}{\arg\min} \, \|\Psi \hat{\boldsymbol{x}}\|_{\mathrm{TV}} \text{ such that } \|\boldsymbol{y} - \Phi \Psi \hat{\boldsymbol{x}}\|_2 \leq \epsilon \, ,$$

  where Ψ represents the inverse spherical harmonic transform and harmonic coefficients are represented by the concatenated vector $\hat{\boldsymbol{x}} \in \mathbb{C}^{L^2}$.

TV inpainting

- Consider inpainting problem $\boldsymbol{y} = \Phi \boldsymbol{x} + \boldsymbol{n}$ in the context of different sampling theorems, where:
  - the samples of f are denoted by the concatenated vector $\boldsymbol{x} \in \mathbb{R}^N$;
  - N is the number of samples on the sphere of the chosen sampling theorem;
  - M noisy measurements $\boldsymbol{y} \in \mathbb{R}^M$ are acquired;
  - the measurement operator $\Phi \in \mathbb{R}^{M \times N}$ represents a random masking of the signal;
  - the noise $\boldsymbol{n} \in \mathbb{R}^M$ is assumed to be iid Gaussian with zero mean.
- Define TV norm on the sphere:

$$\int_{\mathbb{S}^2} \mathrm{d}\Omega \, |\nabla f| \simeq \sum_{t=0}^{N_\theta - 1} \sum_{p=0}^{N_\varphi - 1} |\nabla f| \, q(\theta_t) \simeq \sum_{t=0}^{N_\theta - 1} \sum_{p=0}^{N_\varphi - 1} \sqrt{q^2(\theta_t)(\delta_\theta \boldsymbol{x})^2 + \frac{q^2(\theta_t)}{\sin^2 \theta_t}(\delta_\varphi \boldsymbol{x})^2} \equiv \|\boldsymbol{x}\|_{\mathrm{TV}} \, .$$

- TV inpainting problem solved directly on the sphere:

$$\boldsymbol{x}^\star = \underset{\boldsymbol{x}}{\arg\min} \, \|\boldsymbol{x}\|_{\mathrm{TV}} \;\; \text{such that} \;\; \|\boldsymbol{y} - \Phi \boldsymbol{x}\|_2 \leq \epsilon \, .$$

- TV inpainting problem solved in harmonic space:

$$\hat{\boldsymbol{x}}^\star = \underset{\hat{\boldsymbol{x}}}{\arg\min} \, \|\Psi \hat{\boldsymbol{x}}\|_{\mathrm{TV}} \;\; \text{such that} \;\; \|\boldsymbol{y} - \Phi \Psi \hat{\boldsymbol{x}}\|_2 \leq \epsilon \, ,$$

  where Ψ represents the inverse spherical harmonic transform and harmonic coefficients are represented by the concatenated vector $\hat{\boldsymbol{x}} \in \mathbb{C}^{L^2}$.

TV inpainting: low-resolution simulations

- Solve TV inpainting problem on the sphere in the context of the different sampling theorems.

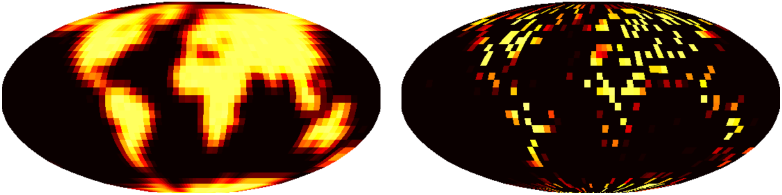

(a) Ground truth

(b) Measurements

Figure: Earth topographic data reconstructed in the harmonic domain for $M/L^2 = 1/2$

TV inpainting: low-resolution simulations

- Solve TV inpainting problem on the sphere in the context of the different sampling theorems.

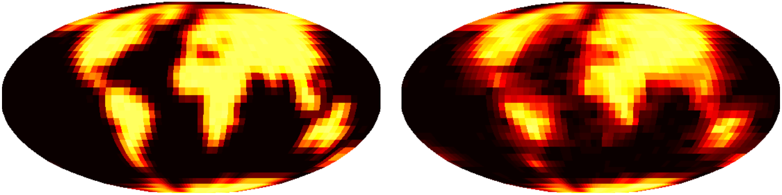

(a) Ground truth

(b) Reconstruction with DH sampling theorem

Figure: Earth topographic data reconstructed in the harmonic domain for $M/L^2 = 1/2$

TV inpainting: low-resolution simulations

- Solve TV inpainting problem on the sphere in the context of the different sampling theorems.

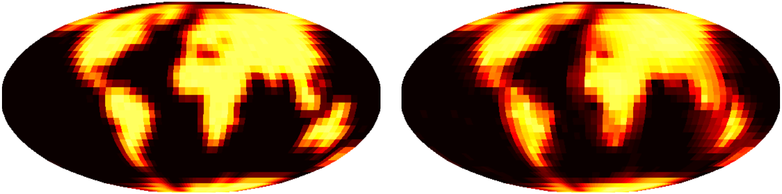

(a) Ground truth (b) Reconstruction with new sampling theorem

Figure: Earth topographic data reconstructed in the harmonic domain for $M/L^2 = 1/2$

TV inpainting: high-resolution simulations

- Require fast adjoint operators as well as fast spherical harmonic transforms to solve optimisation problems.
- Superiority of new sampling theorem clear, hence develop fast adjoints for this case only.

TV inpainting: high-resolution simulations

- Require fast adjoint operators as well as fast spherical harmonic transforms to solve optimisation problems.
- Superiority of new sampling theorem clear, hence develop fast adjoints for this case only.

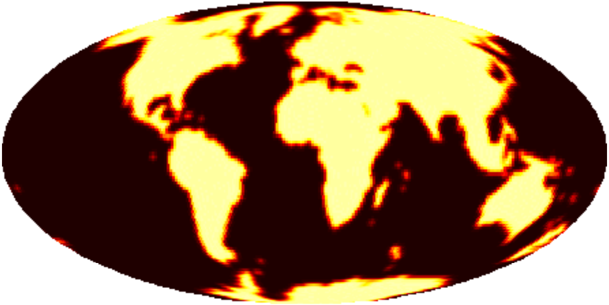

Figure: Ground truth

TV inpainting: high-resolution simulations

- Require fast adjoint operators as well as fast spherical harmonic transforms to solve optimisation problems.
- Superiority of new sampling theorem clear, hence develop fast adjoints for this case only.

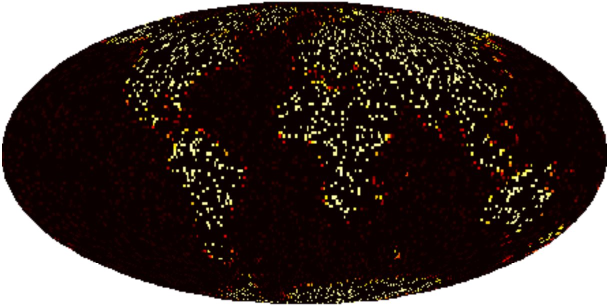

Figure: Measurements $(M/L^2 = 1/4)$

TV inpainting: high-resolution simulations

- Require fast adjoint operators as well as fast spherical harmonic transforms to solve optimisation problems.
- Superiority of new sampling theorem clear, hence develop fast adjoints for this case only.

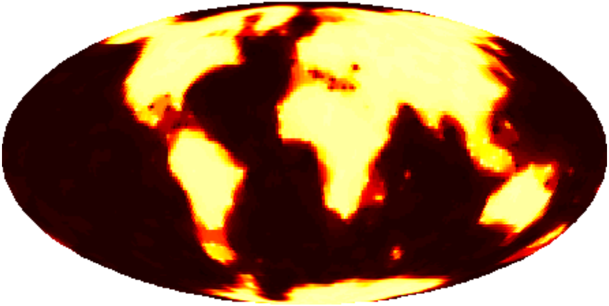

Figure: Reconstruction ($M/L^2 = 1/4$)

Outline

Wavelet transform in Euclidean space

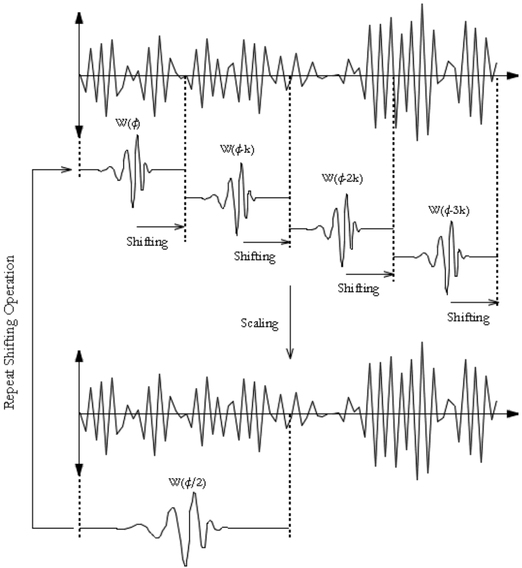

Figure: Wavelet scaling and shifting (image from http://www.wavelet.org/tutorial/)

Wavelet transform in Euclidean space

- Project signal onto wavelets

$$\mathcal{W}^f(a,b) = \langle f, \psi_{a,b} \rangle = |a|^{-1/2} \int_{-\infty}^{\infty} \mathrm{d}t\, f(t)\, \psi^* \left(\frac{t-b}{a} \right),$$

where $\psi_{a,b} = |a|^{-1/2} \psi(\frac{t-b}{a})$.

- Synthesis signal from wavelet coefficients

$$f(t) = C_\psi^{-1} \int_{-\infty}^{\infty} \mathrm{d}b \int_0^{\infty} \frac{\mathrm{d}a}{a^2}\, \mathcal{W}^f(a,b) \psi_{a,b}(t).$$

- Admissibility condition to ensure perfect reconstruction

$$0 < C_\psi \equiv \int_{-\infty}^{\infty} \frac{\mathrm{d}k}{|k|} |\hat{\psi}(k)|^2 < \infty.$$

- Construct on sphere in analogous manner.

Continuous wavelets on the sphere

- First natural wavelet construction on the sphere was derived in the seminal work of Antoine and Vandergheynst (1998) (reintroduced by Wiaux (2005)).
- Construct wavelet atoms from affine transformations (dilation, translation) on the sphere of a mother wavelet.
- The natural extension of translations to the sphere are rotations. Characterised by the elements of the rotation group $\mathrm{SO}(3)$, which parameterise in terms of the three Euler angles $\rho = (\alpha, \beta, \gamma)$. Rotation of a function f on the sphere is defined by

$$[\mathcal{R}(\rho)f](\omega) = f(\rho^{-1}\omega), \quad \rho \in \mathrm{SO}(3) .$$

- How define dilation and admissible wavelets on the sphere?

Continuous wavelets on the sphere

- First natural wavelet construction on the sphere was derived in the seminal work of Antoine and Vandergheynst (1998) (reintroduced by Wiaux (2005)).
- Construct wavelet atoms from affine transformations (dilation, translation) on the sphere of a mother wavelet.
- The natural extension of translations to the sphere are rotations. Characterised by the elements of the rotation group $\mathrm{SO}(3)$, which parameterise in terms of the three Euler angles $\rho = (\alpha, \beta, \gamma)$. Rotation of a function f on the sphere is defined by

$$[\mathcal{R}(\rho) f](\omega) = f(\rho^{-1}\omega), \quad \rho \in \mathrm{SO}(3) \ .$$

- How define dilation and admissible wavelets on the sphere?

Continuous wavelets on the sphere

- First natural wavelet construction on the sphere was derived in the seminal work of Antoine and Vandergheynst (1998) (reintroduced by Wiaux (2005)).
- Construct wavelet atoms from affine transformations (dilation, translation) on the sphere of a mother wavelet.
- The natural extension of translations to the sphere are rotations. Characterised by the elements of the rotation group $\mathrm{SO}(3)$, which parameterise in terms of the three Euler angles $\rho = (\alpha, \beta, \gamma)$. Rotation of a function f on the sphere is defined by

$$[\mathcal{R}(\rho)f](\omega) = f(\rho^{-1}\omega), \quad \rho \in \mathrm{SO}(3) \ .$$

- How define dilation and admissible wavelets on the sphere?

Stereographic projection

- Apply stereographic projection to build an association with the plane.

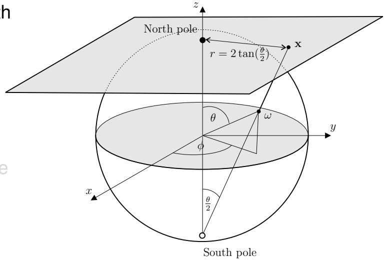

- Stereographic projection operator is defined by $\Pi : \omega \to \boldsymbol{x} = \Pi\omega = (r(\theta), \varphi)$ where $r = 2\tan(\theta/2)$, $\omega \equiv (\theta, \varphi) \in \mathrm{S}^2$ and $\boldsymbol{x} \in \mathbb{R}^2$ is a point in the plane, denoted here by the polar coordinates (r, φ). The inverse operator is $\Pi^{-1} : \boldsymbol{x} \to \omega = \Pi^{-1}\boldsymbol{x} = (\theta(r), \varphi)$, where $\theta(r) = 2\tan^{-1}(r/2)$.

- Define the action of the stereographic projection operator on functions on the plane and sphere. Consider the space of square integrable functions in $\mathrm{L}^2(\mathbb{R}^2, \mathrm{d}^2\boldsymbol{x})$ on the plane and $\mathrm{L}^2(\mathrm{S}^2, \mathrm{d}\Omega(\omega))$ on the sphere.
  - The action of the stereographic projection operator $\Pi : f \in \mathrm{L}^2(\mathrm{S}^2, \mathrm{d}\Omega(\omega)) \to p = \Pi f \in \mathrm{L}^2(\mathbb{R}^2, \mathrm{d}^2\boldsymbol{x})$ on functions is defined as

$$p(r, \varphi) = (\Pi f)(r, \varphi) = (1 + r^2/4)^{-1} f(\theta(r), \varphi) \ .$$

  - The inverse stereographic projection operator $\Pi^{-1} : p \in \mathrm{L}^2(\mathbb{R}^2, \mathrm{d}^2\boldsymbol{x}) \to f = \Pi^{-1} p \in \mathrm{L}^2(\mathrm{S}^2, \mathrm{d}\Omega(\omega))$ on functions is then

$$f(\theta, \varphi) = (\Pi^{-1} p)(\theta, \varphi) = [1 + \tan^2(\theta/2)]\, p(r(\theta), \varphi) \ .$$

Stereographic projection

- Apply stereographic projection to build an association with the plane.

- Stereographic projection operator is defined by $\Pi : \omega \to \boldsymbol{x} = \Pi\omega = (r(\theta), \varphi)$ where $r = 2\tan(\theta/2)$, $\omega \equiv (\theta, \varphi) \in \mathrm{S}^2$ and $\boldsymbol{x} \in \mathbb{R}^2$ is a point in the plane, denoted here by the polar coordinates (r, φ). The inverse operator is $\Pi^{-1} : \boldsymbol{x} \to \omega = \Pi^{-1}\boldsymbol{x} = (\theta(r), \varphi)$, where $\theta(r) = 2\tan^{-1}(r/2)$.

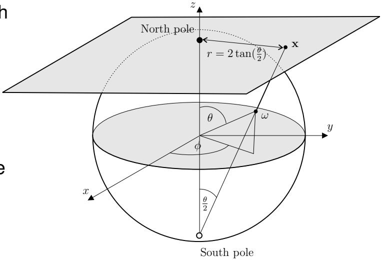

- Define the action of the stereographic projection operator on functions on the plane and sphere. Consider the space of square integrable functions in $\mathrm{L}^2(\mathbb{R}^2, \mathrm{d}^2\boldsymbol{x})$ on the plane and $\mathrm{L}^2(\mathrm{S}^2, \mathrm{d}\Omega(\omega))$ on the sphere.
  - The action of the stereographic projection operator $\Pi : f \in \mathrm{L}^2(\mathrm{S}^2, \mathrm{d}\Omega(\omega)) \to p = \Pi f \in \mathrm{L}^2(\mathbb{R}^2, \mathrm{d}^2\boldsymbol{x})$ on functions is defined as

$$p(r, \varphi) = (\Pi f)(r, \varphi) = (1 + r^2/4)^{-1} f(\theta(r), \varphi) .$$

  - The inverse stereographic projection operator $\Pi^{-1} : p \in \mathrm{L}^2(\mathbb{R}^2, \mathrm{d}^2\boldsymbol{x}) \to f = \Pi^{-1} p \in \mathrm{L}^2(\mathrm{S}^2, \mathrm{d}\Omega(\omega))$ on functions is then

$$f(\theta, \varphi) = (\Pi^{-1} p)(\theta, \varphi) = [1 + \tan^2(\theta/2)] p(r(\theta), \varphi) .$$

Stereographic projection

- Apply stereographic projection to build an association with the plane.

- Stereographic projection operator is defined by $\Pi : \omega \rightarrow \boldsymbol{x} = \Pi\omega = (r(\theta), \varphi)$ where $r = 2\tan(\theta/2)$, $\omega \equiv (\theta, \varphi) \in \mathrm{S}^2$ and $\boldsymbol{x} \in \mathbb{R}^2$ is a point in the plane, denoted here by the polar coordinates (r, φ). The inverse operator is $\Pi^{-1} : \boldsymbol{x} \rightarrow \omega = \Pi^{-1}\boldsymbol{x} = (\theta(r), \varphi)$, where $\theta(r) = 2\tan^{-1}(r/2)$.

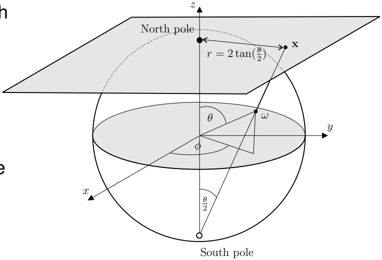

- Define the action of the stereographic projection operator on functions on the plane and sphere. Consider the space of square integrable functions in $\mathrm{L}^2(\mathbb{R}^2, \mathrm{d}^2\boldsymbol{x})$ on the plane and $\mathrm{L}^2(\mathrm{S}^2, \mathrm{d}\Omega(\omega))$ on the sphere.
  - The action of the stereographic projection operator $\Pi : f \in \mathrm{L}^2(\mathrm{S}^2, \mathrm{d}\Omega(\omega)) \rightarrow p = \Pi f \in \mathrm{L}^2(\mathbb{R}^2, \mathrm{d}^2\boldsymbol{x})$ on functions is defined as

$$p(r, \varphi) = (\Pi f)(r, \varphi) = (1 + r^2/4)^{-1} f(\theta(r), \varphi) \; .$$

  - The inverse stereographic projection operator $\Pi^{-1} : p \in \mathrm{L}^2(\mathbb{R}^2, \mathrm{d}^2\boldsymbol{x}) \rightarrow f = \Pi^{-1}p \in \mathrm{L}^2(\mathrm{S}^2, \mathrm{d}\Omega(\omega))$ on functions is then

$$f(\theta, \varphi) = (\Pi^{-1}p)(\theta, \varphi) = [1 + \tan^2(\theta/2)]\, p(r(\theta), \varphi) \; .$$

Dilation on the sphere

- The spherical dilation operator $\mathcal{D}(a) : f(\omega) \rightarrow [\mathcal{D}(a)f](\omega)$ in $\mathrm{L}^2(\mathrm{S}^2,\, \mathrm{d}\Omega(\omega))$ is defined as the conjugation by Π of the Euclidean dilation $d(a)$ in $\mathrm{L}^2(\mathbb{R}^2,\, \mathrm{d}^2\boldsymbol{x})$ on tangent plane at north pole:

$$\mathcal{D}(a) \equiv \Pi^{-1}\, d(a)\, \Pi \; .$$

- Spherical dilation given by

$$[\mathcal{D}(a)f](\omega) = [\lambda(a, \theta, \varphi)]^{1/2} f(\omega_{1/a}) \; ,$$

where $\omega_a = (\theta_a, \varphi)$ and $\tan(\theta_a/2) = a \tan(\theta/2)$.

- Cocycle of a spherical dilation is defined by

$$\lambda(a, \theta, \varphi) \equiv \frac{4a^2}{[(a^2-1)\cos\theta + (a^2+1)]^2} \; .$$

Wavelet analysis formula

- Wavelets on the sphere may now be constructed from rotations and dilations of a mother spherical wavelet $\Phi \in \mathrm{L}^2(\mathrm{S}^2, \, \mathrm{d}\Omega(\omega))$. The corresponding wavelet family $\{\Phi_{a,\rho} \equiv \mathcal{R}(\rho)\mathcal{D}(a)\Phi : \rho \in \mathrm{SO}(3), \, a \in \mathbb{R}_*^+\}$ provides an over-complete set of functions in $\mathrm{L}^2(\mathrm{S}^2, \, \mathrm{d}\Omega(\omega))$.
- The CSWT of $f \in \mathrm{L}^2(\mathrm{S}^2, \, \mathrm{d}\Omega(\omega))$ is given by the projection on to each wavelet atom in the usual manner:

$$\widehat{\mathcal{W}}_{\Phi}^{f}(a, \rho) = \langle f, \Phi_{a,\rho} \rangle = \int_{\mathrm{S}^2} \mathrm{d}\Omega(\omega) \, f(\omega) \, \Phi_{a,\rho}^{*}(\omega) \; ,$$

where $\mathrm{d}\Omega(\omega) = \sin\theta \, \mathrm{d}\theta \, \mathrm{d}\varphi$ is the usual invariant measure on the sphere.

- Transform general in the sense that all orientations in the rotation group $\mathrm{SO}(3)$ are considered, thus directional structure is naturally incorporated.
- Fast algorithms essential (for a review see Wiaux, JDM & Vielva 2007)
  - Factoring of rotations: JDM *et al.* (2007), Wandelt & Gorski (2001)
  - Separation of variables: Wiaux *et al.* (2005)

Wavelet analysis formula

- Wavelets on the sphere may now be constructed from rotations and dilations of a mother spherical wavelet $\Phi \in \mathrm{L}^2(\mathrm{S}^2, \mathrm{d}\Omega(\omega))$. The corresponding wavelet family $\{\Phi_{a,\rho} \equiv \mathcal{R}(\rho)\mathcal{D}(a)\Phi : \rho \in \mathrm{SO}(3), a \in \mathbb{R}_*^+\}$ provides an over-complete set of functions in $\mathrm{L}^2(\mathrm{S}^2, \mathrm{d}\Omega(\omega))$.
- The CSWT of $f \in \mathrm{L}^2(\mathrm{S}^2, \mathrm{d}\Omega(\omega))$ is given by the projection on to each wavelet atom in the usual manner:

$$\widehat{\mathcal{W}}_{\Phi}^{f}(a, \rho) = \langle f, \Phi_{a,\rho} \rangle = \int_{\mathrm{S}^2} \mathrm{d}\Omega(\omega)\, f(\omega)\, \Phi_{a,\rho}^{*}(\omega) \ ,$$

  where $\mathrm{d}\Omega(\omega) = \sin\theta \,\mathrm{d}\theta \,\mathrm{d}\varphi$ is the usual invariant measure on the sphere.
- Transform general in the sense that all orientations in the rotation group $\mathrm{SO}(3)$ are considered, thus directional structure is naturally incorporated.
- Fast algorithms essential (for a review see Wiaux, JDM & Vielva 2007)
  - Factoring of rotations: JDM *et al.* (2007), Wandelt & Gorski (2001)
  - Separation of variables: Wiaux *et al.* (2005)

Wavelet analysis formula

- Wavelets on the sphere may now be constructed from rotations and dilations of a mother spherical wavelet $\Phi \in \mathrm{L}^2(\mathrm{S}^2, \,\mathrm{d}\Omega(\omega))$. The corresponding wavelet family $\{\Phi_{a,\rho} \equiv \mathcal{R}(\rho)\mathcal{D}(a)\Phi : \rho \in \mathrm{SO}(3), \, a \in \mathbb{R}_*^+\}$ provides an over-complete set of functions in $\mathrm{L}^2(\mathrm{S}^2, \,\mathrm{d}\Omega(\omega))$.
- The CSWT of $f \in \mathrm{L}^2(\mathrm{S}^2, \,\mathrm{d}\Omega(\omega))$ is given by the projection on to each wavelet atom in the usual manner:

$$\widehat{\mathcal{W}}_{\Phi}^{f}(a, \rho) = \langle f, \Phi_{a,\rho} \rangle = \int_{\mathrm{S}^2} \mathrm{d}\Omega(\omega)\, f(\omega)\, \Phi_{a,\rho}^{*}(\omega) \ ,$$

  where $\mathrm{d}\Omega(\omega) = \sin\theta \,\mathrm{d}\theta \,\mathrm{d}\varphi$ is the usual invariant measure on the sphere.
- Transform general in the sense that all orientations in the rotation group $\mathrm{SO}(3)$ are considered, thus directional structure is naturally incorporated.
- Fast algorithms essential (for a review see Wiaux, JDM & Vielva 2007)
  - Factoring of rotations: JDM *et al.* (2007), Wandelt & Gorski (2001)
  - Separation of variables: Wiaux *et al.* (2005)

Wavelet synthesis formula

- The synthesis of a signal on the sphere from its wavelet coefficients is given by

$$f(\omega) = \int_0^\infty \frac{\mathrm{d}a}{a^3} \int_{\mathrm{SO}(3)} \mathrm{d}\varrho(\rho) \widehat{\mathcal{W}}^f_\Phi(a,\rho) \, [\mathcal{R}(\rho)\widehat{L}_\Phi \Phi_a](\omega) \, ,$$

  where $\mathrm{d}\varrho(\rho) = \sin\beta \, \mathrm{d}\alpha \, \mathrm{d}\beta \, \mathrm{d}\gamma$ is the invariant measure on the rotation group $\mathrm{SO}(3)$.

- The $\widehat{L}_\Phi$ operator in $\mathrm{L}^2(\mathrm{S}^2, \, \mathrm{d}\Omega(\omega))$ is defined by the action

$$(\widehat{L}_\Phi g)_{\ell m} \equiv g_{\ell m} / \widehat{C}^\ell_\Phi$$

  on the spherical harmonic coefficients of functions $g \in \mathrm{L}^2(\mathrm{S}^2, \, \mathrm{d}\Omega(\omega))$.

- In order to ensure the perfect reconstruction of a signal synthesised from its wavelet coefficients, the admissibility condition

$$0 < \widehat{C}^\ell_\Phi \equiv \frac{8\pi^2}{2\ell+1} \sum_{m=-\ell}^{\ell} \int_0^\infty \frac{\mathrm{d}a}{a^3} \mid (\Phi_a)_{\ell m} \mid^2 < \infty$$

  must be satisfied for all $\ell \in \mathbb{N}$, where $(\Phi_a)_{\ell m}$ are the spherical harmonic coefficients of $\Phi_a(\omega)$.

Wavelet synthesis formula

- The synthesis of a signal on the sphere from its wavelet coefficients is given by

$$f(\omega) = \int_0^\infty \frac{\mathrm{d}a}{a^3} \int_{\mathrm{SO}(3)} \mathrm{d}\varrho(\rho) \widehat{\mathcal{W}}^f_\Phi(a,\rho) \, [\mathcal{R}(\rho)\widehat{L}_\Phi \Phi_a](\omega) \, ,$$

  where $\mathrm{d}\varrho(\rho) = \sin\beta \, \mathrm{d}\alpha \, \mathrm{d}\beta \, \mathrm{d}\gamma$ is the invariant measure on the rotation group $\mathrm{SO}(3)$.

- The $\widehat{L}_\Phi$ operator in $\mathrm{L}^2(\mathrm{S}^2, \mathrm{d}\Omega(\omega))$ is defined by the action

$$(\widehat{L}_\Phi g)_{\ell m} \equiv g_{\ell m} / \widehat{C}^\ell_\Phi$$

  on the spherical harmonic coefficients of functions $g \in \mathrm{L}^2(\mathrm{S}^2, \mathrm{d}\Omega(\omega))$.

- In order to ensure the perfect reconstruction of a signal synthesised from its wavelet coefficients, the admissibility condition

$$0 < \widehat{C}^\ell_\Phi \equiv \frac{8\pi^2}{2\ell+1} \sum_{m=-\ell}^{\ell} \int_0^\infty \frac{\mathrm{d}a}{a^3} \mid (\Phi_a)_{\ell m} \mid^2 < \infty$$

  must be satisfied for all $\ell \in \mathbb{N}$, where $(\Phi_a)_{\ell m}$ are the spherical harmonic coefficients of $\Phi_a(\omega)$.

Correspondence principle

- Correspondence principle between spherical and Euclidean wavelets states that the inverse stereographic projection of an *admissible* wavelet on the plane yields an *admissible* wavelet on the sphere (proved by Wiaux *et al.* 2005)
- Mother wavelets on sphere constructed from the projection of mother Euclidean wavelets defined on the plane:

$$\Phi = \Pi^{-1}\Phi_{\mathbb{R}^2} ,$$

where $\Phi_{\mathbb{R}^2} \in L^2(\mathbb{R}^2, d^2\boldsymbol{x})$ is an admissible wavelet in the plane.

- Directional wavelets on sphere may be naturally constructed in this setting – they are simply the projection of directional Euclidean planar wavelets on to the sphere.

Correspondence principle

- Correspondence principle between spherical and Euclidean wavelets states that the inverse stereographic projection of an *admissible* wavelet on the plane yields an *admissible* wavelet on the sphere (proved by Wiaux *et al.* 2005)
- Mother wavelets on sphere constructed from the projection of mother Euclidean wavelets defined on the plane:

$$\Phi = \Pi^{-1}\Phi_{\mathbb{R}^2} \ ,$$

where $\Phi_{\mathbb{R}^2} \in \mathrm{L}^2(\mathbb{R}^2, \, \mathrm{d}^2\boldsymbol{x})$ is an admissible wavelet in the plane.

- Directional wavelets on sphere may be naturally constructed in this setting – they are simply the projection of directional Euclidean planar wavelets on to the sphere.

Correspondence principle

- Correspondence principle between spherical and Euclidean wavelets states that the inverse stereographic projection of an *admissible* wavelet on the plane yields an *admissible* wavelet on the sphere (proved by Wiaux *et al.* 2005)
- Mother wavelets on sphere constructed from the projection of mother Euclidean wavelets defined on the plane:

$$\Phi = \Pi^{-1} \Phi_{\mathbb{R}^2} \ ,$$

  where $\Phi_{\mathbb{R}^2} \in \mathrm{L}^2(\mathbb{R}^2, \, \mathrm{d}^2\boldsymbol{x})$ is an admissible wavelet in the plane.
- Directional wavelets on sphere may be naturally constructed in this setting – they are simply the projection of directional Euclidean planar wavelets on to the sphere.

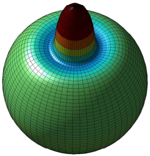

(a) SMHW

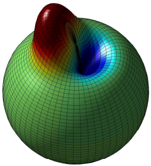

(b) SBW

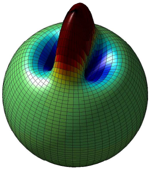

(c) S2GDW

Figure: Spherical wavelets at scale $a, b = 0.2$.

Scale-discretised wavelets

- Wiaux, JDM, Vandergheynst, Blanc (2008)
  Exact reconstruction with directional wavelets on the sphere

- Dilation performed in harmonic space.

- The scale-discretised wavelet $\Gamma \in \mathrm{L}^2(\mathrm{S}^2, \mathrm{d}\Omega)$ is defined in harmonic space:

$$\widehat{\Gamma}_{\ell m} = \tilde{K}_\Gamma(\ell) S^\Gamma_{\ell m} \ .$$

- Construct wavelets to satisfy a resolution of the identity for $0 \leq \ell < L$:

$$\tilde{\Phi}^2_\Gamma(\alpha^J \ell) + \sum_{j=0}^{J} \tilde{K}^2_\Gamma(\alpha^j \ell) = 1 \ .$$

Scale-discretised wavelets

- Wiaux, JDM, Vandergheynst, Blanc (2008)
  Exact reconstruction with directional wavelets on the sphere

- Dilation performed in harmonic space.
- The scale-discretised wavelet $\Gamma \in \mathrm{L}^2(\mathrm{S}^2, \mathrm{d}\Omega)$ is defined in harmonic space:

$$\widehat{\Gamma}_{\ell m} = \tilde{K}_\Gamma(\ell) S^\Gamma_{\ell m} \ .$$

- Construct wavelets to satisfy a resolution of the identity for $0 \leq \ell < L$:

$$\tilde{\Phi}^2_\Gamma(\alpha^J \ell) + \sum_{j=0}^{J} \tilde{K}^2_\Gamma(\alpha^j \ell) = 1 \ .$$

Scale-discretised wavelets

- Wiaux, JDM, Vandergheynst, Blanc (2008)
  Exact reconstruction with directional wavelets on the sphere

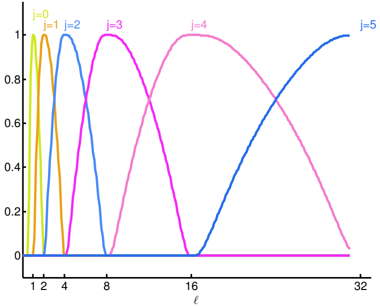

Figure: Harmonic tiling on the sphere.

- Dilation performed in harmonic space.
- The scale-discretised wavelet $\Gamma \in \mathrm{L}^2(\mathrm{S}^2, \mathrm{d}\Omega)$ is defined in harmonic space:

$$\widehat{\Gamma}_{\ell m} = \tilde{K}_\Gamma(\ell) S^\Gamma_{\ell m} \, .$$

- Construct wavelets to satisfy a resolution of the identity for $0 \leq \ell < L$:

$$\tilde{\Phi}^2_\Gamma(\alpha^J \ell) + \sum_{j=0}^{J} \tilde{K}^2_\Gamma(\alpha^j \ell) = 1 .$$

Scale-discretised wavelets

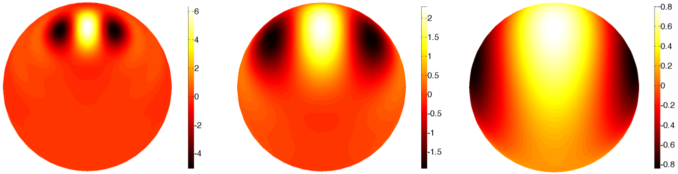

Figure: Spherical scale-discretised wavelets.

- The scale-discretised wavelet transform is given by the usual projection onto each wavelet:

$$W_{\Gamma}^{F}(\rho, \alpha^{j}) = \langle F, \Gamma_{\rho, \alpha^{j}} \rangle = \int_{S^2} \mathrm{d}\Omega(\omega)\, F(\omega)\, \Gamma^{*}_{\rho, \alpha^{j}}(\omega)\ .$$

- The original function may be recovered exactly in practice from the wavelet (and scaling) coefficients:

$$F(\omega) = [\Phi_{\alpha^J} F](\omega) + \sum_{j=0}^{J} \int_{\mathrm{SO(3)}} \mathrm{d}\rho\, W_{\Gamma}^{F}\left(\rho, \alpha^{j}\right) \left[R(\rho)\, L^{\mathrm{d}} \Gamma_{\alpha^{j}}\right](\omega)\ ,$$

where the operator L^{d} is defined by the following action on the spherical harmonic coefficients of functions: $\widehat{L^{\mathrm{d}} G}_{lm} = (2l+1)\widehat{G}_{lm}/8\pi^2$.

Scale-discretised wavelets

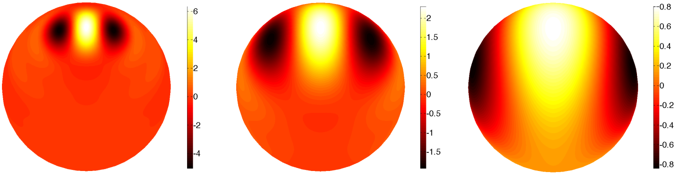

Figure: Spherical scale-discretised wavelets.

- The scale-discretised wavelet transform is given by the usual projection onto each wavelet:

$$W_\Gamma^F(\rho, \alpha^j) = \langle F, \Gamma_{\rho,\alpha^j} \rangle = \int_{S^2} \mathrm{d}\Omega(\omega)\, F(\omega)\, \Gamma^*_{\rho,\alpha^j}(\omega) \, .$$

- The original function may be recovered exactly in practice from the wavelet (and scaling) coefficients:

$$F(\omega) = \left[\Phi_{\alpha^J} F\right](\omega) + \sum_{j=0}^{J} \int_{\mathrm{SO(3)}} \mathrm{d}\rho\, W_\Gamma^F\left(\rho, \alpha^j\right) \left[R(\rho)\, L^{\mathrm{d}} \Gamma_{\alpha^j}\right](\omega) \, ,$$

where the operator L^{d} is defined by the following action on the spherical harmonic coefficients of functions: $\widehat{L^{\mathrm{d}} G}_{lm} = (2l+1)\widehat{G}_{lm}/8\pi^2$.

Scale-discretised wavelets

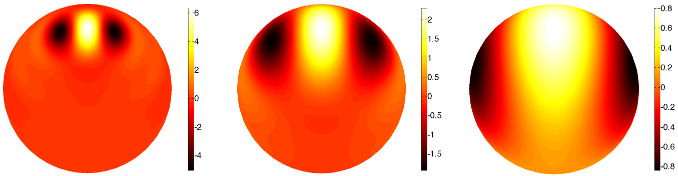

Figure: Spherical scale-discretised wavelets.

- The scale-discretised wavelet transform is given by the usual projection onto each wavelet:

$$W_\Gamma^F(\rho, \alpha^j) = \langle F, \Gamma_{\rho,\alpha^j} \rangle = \int_{S^2} d\Omega(\omega)\, F(\omega)\, \Gamma^*_{\rho,\alpha^j}(\omega)\ .$$

- The original function may be recovered exactly in practice from the wavelet (and scaling) coefficients:

$$F(\omega) = [\Phi_{\alpha^J} F](\omega) + \sum_{j=0}^{J} \int_{\mathrm{SO(3)}} d\rho\, W_\Gamma^F\left(\rho, \alpha^j\right) \left[R(\rho)\, L^{\mathrm{d}} \Gamma_{\alpha^j}\right](\omega)\ ,$$

where the operator L^{d} is defined by the following action on the spherical harmonic coefficients of functions: $\widehat{L^{\mathrm{d}} G}_{lm} = (2l+1)\widehat{G}_{lm}/8\pi^2$.

Outline

Data on the three-ball (solid sphere)

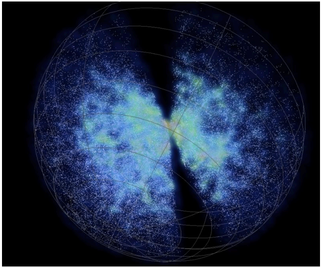

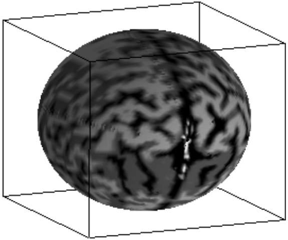

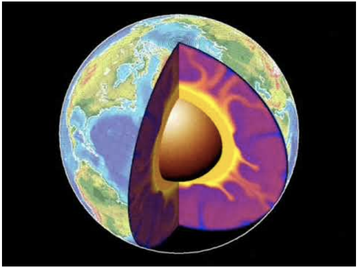

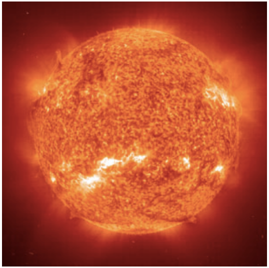

Wavelets on the ball

- Boris Leistedt & JDM (2012), *Exact wavelets on the solid sphere*, in preparation.

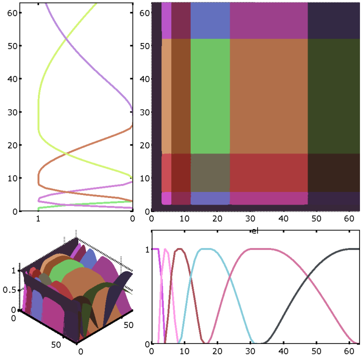

Figure: Harmonic tiling on the ball.

$$W^{\Psi^{jj'}}(r,\omega) = \langle f, T_r R_\omega \Psi^{jj'} \rangle = (f \star \Psi^{jj'})(r,\omega) = \int_{\mathcal{B}^3_{\mathbb{R}+}} \mathrm{d}^3\boldsymbol{r}' \, f(\boldsymbol{r}') \, (T_r R_\omega \Psi^{jj'})^*(\boldsymbol{r}')$$

$$f(r,\omega) = \int_{\mathcal{B}^3_{\mathbb{R}+}} \mathrm{d}^3\boldsymbol{r}' \, W^{\Phi}(\boldsymbol{r}') \, (T_r R_\omega \Phi)(\boldsymbol{r}') + \sum_{jj'} \int_{\mathcal{B}^3_{\mathbb{R}+}} \mathrm{d}^3\boldsymbol{r}' \, W^{\Psi^{jj'}}(\boldsymbol{r}') \, (T_r R_\omega \Psi^{jj'})(\boldsymbol{r}').$$

Wavelets on the ball

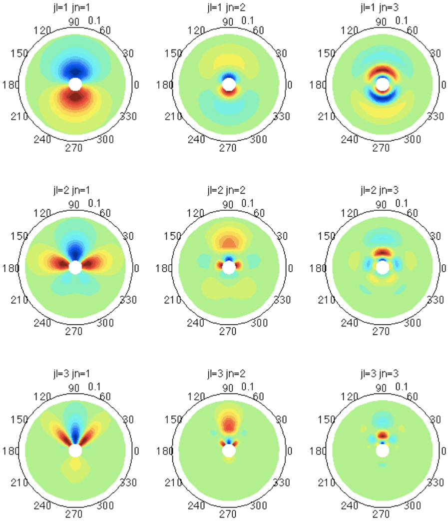

Figure: Wavelets on the ball.

Summary

Upcoming publication

B. Leistedt & JDM, *Exact wavelets on the solid sphere*, IEEE Trans. Sig. Proc., in preparation.

Codes

- **SSHT** Code to compute exact (spin) spherical harmonic transforms based on the new sampling theorem (Fortran, C, Matlab).
- **FastCSWT** Code to compute fast continuous wavelet transforms (forward transform only) using the fast convolution of Wandelt & Gorski (2001) (Fortran).
- **S2DW** Code to compute fast scale-discretised wavelet transforms on the sphere (Fortran).
- **S2LET** Code to compute fast scale-discretised wavelet transforms on the sphere (Fortran, C, Matlab) [TO APPEAR].
- **B3LET** Code to compute fast scale-discretised wavelet transforms on the solid sphere (Fortran, C, Matlab) [TO APPEAR].

All codes available under the GPL from `http://www.jasonmcewen.org/`

Dark energy

- Universe consists of ordinary baryonic matter, cold dark matter and dark energy.
- Dark energy represents energy density of empty space. Modelled by a cosmological fluid with negative pressure acting as a repulsive force.
- Evidence for dark energy provided by observations of CMB, supernovae and large scale structure of Universe.

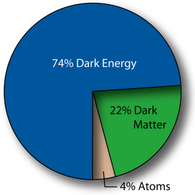

Credit: WMAP Science Team

- However, a consistent model in the framework of particle physics lacking. Indeed, attempts to predict a cosmological constant obtain a value that is too large by a factor of $\sim 10^{120}$.
- Dark energy dominates our Universe but yet we know very little about its nature and origin.
- Verification of dark energy by independent physical methods of considerable interest.
- Independent methods may also prove more sensitive probes of properties of dark energy.

Dark energy

- Universe consists of ordinary baryonic matter, cold dark matter and dark energy.
- Dark energy represents energy density of empty space. Modelled by a cosmological fluid with negative pressure acting as a repulsive force.
- Evidence for dark energy provided by observations of CMB, supernovae and large scale structure of Universe.

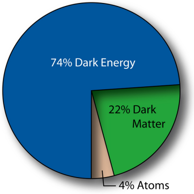

Credit: WMAP Science Team

- However, a consistent model in the framework of particle physics lacking. Indeed, attempts to predict a cosmological constant obtain a value that is too large by a factor of $\sim 10^{120}$.
- Dark energy dominates our Universe but yet we know very little about its nature and origin.
- Verification of dark energy by independent physical methods of considerable interest.
- Independent methods may also prove more sensitive probes of properties of dark energy.

Dark energy

- Universe consists of ordinary baryonic matter, cold dark matter and dark energy.
- Dark energy represents energy density of empty space. Modelled by a cosmological fluid with negative pressure acting as a repulsive force.
- Evidence for dark energy provided by observations of CMB, supernovae and large scale structure of Universe.

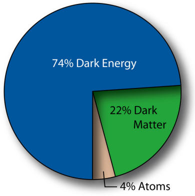

Credit: WMAP Science Team

- However, a consistent model in the framework of particle physics lacking. Indeed, attempts to predict a cosmological constant obtain a value that is too large by a factor of $\sim 10^{120}$.
- Dark energy dominates our Universe but yet we know very little about its nature and origin.
- Verification of dark energy by independent physical methods of considerable interest.
- Independent methods may also prove more sensitive probes of properties of dark energy.

Integrated Sachs-Wolfe (ISW) effect

(ball sim constant movie) (ball sim evolving movie)

Figure: ISW effect analogy

- CMB photons blue (red) shifted when fall into (out of) potential wells.
- Evolution of potential during photon propagation $\rightarrow$ net change in photon energy.
- Gravitation potentials constant w.r.t. conformal time in matter dominated universe.
- Deviation from matter domination due to curvature or dark energy causes potentials to evolve with time $\rightarrow$ secondary anisotropy induced in CMB.

Detecting the ISW effect

- WMAP shown universe is (nearly) flat.
- Detection of ISW effect $\Rightarrow$ direct evidence for dark energy.
- Cannot isolate the ISW signal from CMB anisotropies easily.
- Instead, detect by cross-correlating CMB anisotropies with tracers of large scale structure.
(Crittenden & Turok 1996
- Wavelets ideal analysis tool to search for correlation induced by ISW effect since signal manifest at different scales and locations.
(Pioneered by Vielva *et al.* 2005, followed by JDM *et al.* 2006, JDM *et al.* 2007 and others.)
- Compute correlation of WMAP and NVSS radio galaxy survey and compare to Monte Carlo simulations to determine significance of any candidate detections.

Detecting the ISW effect

- WMAP shown universe is (nearly) flat.
- Detection of ISW effect $\Rightarrow$ direct evidence for dark energy.
- Cannot isolate the ISW signal from CMB anisotropies easily.
- Instead, detect by cross-correlating CMB anisotropies with tracers of large scale structure.
  (Crittenden & Turok 1996
- Wavelets ideal analysis tool to search for correlation induced by ISW effect since signal manifest at different scales and locations.
  (Pioneered by Vielva *et al.* 2005, followed by JDM *et al.* 2006, JDM *et al.* 2007 and others.)
- Compute correlation of WMAP and NVSS radio galaxy survey and compare to Monte Carlo simulations to determine significance of any candidate detections.

Detecting the ISW effect

- WMAP shown universe is (nearly) flat.
- Detection of ISW effect $\Rightarrow$ direct evidence for dark energy.
- Cannot isolate the ISW signal from CMB anisotropies easily.
- Instead, detect by cross-correlating CMB anisotropies with tracers of large scale structure.
  (Crittenden & Turok 1996
- Wavelets ideal analysis tool to search for correlation induced by ISW effect since signal manifest at different scales and locations.
  (Pioneered by Vielva *et al.* 2005, followed by JDM *et al.* 2006, JDM *et al.* 2007 and others.)
- Compute correlation of WMAP and NVSS radio galaxy survey and compare to Monte Carlo simulations to determine significance of any candidate detections.

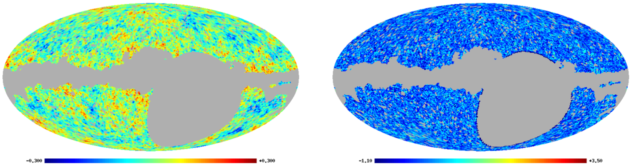

(a) WMAP (b) NVSS

Figure: WMAP and NVSS maps after application of the joint mask

Detection of the ISW effect with wavelets

- Significant correlation detected between the WMAP and NVSS data.
- Foreground contamination and instrumental systematics ruled out as source of the correlation $\Rightarrow$ correlation due to ISW effect.
- Direct observational evidence for dark energy.

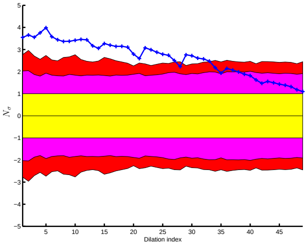

Figure: Wavelet correlation

Detection of the ISW effect with wavelets

- Significant correlation detected between the WMAP and NVSS data.
- Foreground contamination and instrumental systematics ruled out as source of the correlation $\Rightarrow$ correlation due to ISW effect.
- Direct observational evidence for dark energy.

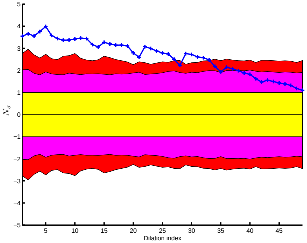

Figure: Wavelet correlation

Constraining dark energy with wavelets

- Possible to use positive detection of the ISW effect to constrain parameters of cosmological models that describe dark energy:
  - Proportional energy density Ω_Λ.
  - Equation of state parameter w relating pressure and density of cosmological fluid that models dark energy, *i.e.* $p = w\rho$.
- Parameter estimates of $\Omega_\Lambda = 0.63^{+0.18}_{-0.17}$ and $w = -0.77^{+0.35}_{-0.36}$ computed from the mean of the marginalised distributions (consistent with other analysis techniques and data sets).

Constraining dark energy with wavelets

- Possible to use positive detection of the ISW effect to constrain parameters of cosmological models that describe dark energy:
  - Proportional energy density Ω_Λ.
  - Equation of state parameter w relating pressure and density of cosmological fluid that models dark energy, *i.e.* $p = w\rho$.
- Parameter estimates of $\Omega_\Lambda = 0.63^{+0.18}_{-0.17}$ and $w = -0.77^{+0.35}_{-0.36}$ computed from the mean of the marginalised distributions (consistent with other analysis techniques and data sets).

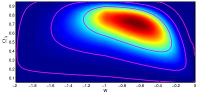

(a) Full likelihood surface

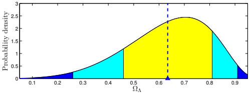

(b) Marginalised distribution for Ω_Λ

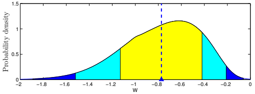

(c) Marginalised distribution for w

Figure: Dark energy likelihoods